

Analysis of the ghost and mirror fields in the Nernst signal induced by superconducting fluctuationsA. Glatz ^{1,2}, A. Pourret ³, and A. A. Varlamov ⁴¹*Materials Science Division, Argonne National Laboratory, 9700 South Cass Avenue, Argonne, Illinois 60639, USA*²*Department of Physics, Northern Illinois University, DeKalb, Illinois 60115, USA*³*Université Grenoble Alpes, CEA, IRIG, PHELIQS, F-38000 Grenoble, France*⁴*CNR-SPIN, c/o DICII-Università di Roma Tor Vergata, Via del Politecnico 1, I-00133 Rome, Italy*

(Received 20 July 2020; revised 23 October 2020; accepted 4 November 2020; published 20 November 2020)

We present a complete analysis of the Nernst signal due to superconducting fluctuations in a large variety of superconductors from conventional to unconventional ones. A closed analytical expression of the fluctuation contribution to the Nernst signal is obtained in a large range of temperature and magnetic field. We apply this expression directly to experimental measurements of the Nernst signal in $\text{Nb}_x\text{Si}_{1-x}$ thin films and URu_2Si_2 superconductors. Both magnetic field and temperature dependence of the available data are fitted with very good accuracy using only two fitting parameters, the superconducting temperature T_{c0} and the upper critical field $H_{c2}(0)$. The obtained values agree very well with experimentally obtained values. We also extract the ghost lines (the maximum of the Nernst signal for constant temperature or magnetic field) from the complete expression and also compare it to several experimentally obtained curves. Our approach predicts a linear temperature dependence for the ghost critical field well above T_{c0} . Within the errors of the experimental data, this linearity is indeed observed in many superconductors far from T_{c0} .

DOI: [10.1103/PhysRevB.102.174507](https://doi.org/10.1103/PhysRevB.102.174507)**I. INTRODUCTION**

In a superconductor above its critical temperature T_{c0} , global superconducting coherence vanishes, leaving behind droplets of short-lived Cooper pairs. Superconducting fluctuations, discovered in the late 1960s, have constituted an important research area in superconductivity as they manifest in a variety of phenomena. Today, their investigation has emerged as a powerful tool for quantifying material parameters of new superconductors. In this regard, the observation of a giant Nernst signal (three orders of magnitude larger than the value of the corresponding coefficient in typical metals) over a wide range of temperatures and magnetic fields attracted great attention from the superconductivity community and caused lively theoretical discussions [1–6]. Important milestones were its discovery in underdoped phases of high-temperature superconductors [7], later in the normal phase of conventional superconductors [8,9], and in normal phases of the overdoped, optimally doped, and underdoped superconductors $\text{La}_{1.8-x}\text{Eu}_{0.2}\text{Sr}_x\text{CuO}_4$ and $\text{Pr}_{2-x}\text{Ce}_x\text{CuO}_4$ [10] and, finally, the observation of the colossal thermomagnetic response in the exotic heavy-fermion superconductor URu_2Si_2 [11]. Today, it is commonly agreed that this effect is related to superconducting fluctuations, and its profound relationship to the fluctuation magnetization is well established [10,12,13].

One of the characteristic features of the fluctuation-induced Nernst signal is its nonmonotonous dependence on applied magnetic fields. The latter follows from very generic heuristic arguments: the fluctuation-induced Nernst signal is the response to an applied crossed magnetic field and temperature gradient, $\mathfrak{N}^{(fl)} = \beta_{xy}^{(fl)} R_{\square}$, where $\beta_{xy}^{(fl)}$ is the off-diagonal component of the fluctuation-induced contribution to the ther-

moelectric tensor [14] and R_{\square} is the film sheet resistance. Hence, it is zero at $H = 0$ (where the thermoelectric tensor is diagonal), and it should vanish in very strong fields, which suppress fluctuations [14]. Indeed, a maximum of the Nernst signal as a function of the magnetic field has been widely observed [8–11]. The study of the temperature dependence of the field at which the Nernst signal is maximum, the *ghost (critical) field* $H^*(T)$, acquired special significance for HTS compounds since the authors of Refs. [10,11] proposed to use it for the precise determination of the second critical field $H_{c2}(0)$, often inaccessible for direct measurements because of its huge value.

Here we carefully analyze the behavior of the maximum in the Nernst signal both in the two $\text{Nb}_x\text{Si}_{1-x}$ samples we measured and in available data on superconductors of different classes. For this purpose, we developed numerical fluctuation spectroscopy [13] for the fluctuation Nernst signal based on the complete expression for the Nernst signal, which includes all fluctuation corrections [2]. This allows us to not only extract real material parameters like the BCS critical temperature T_{c0} and the critical magnetic field $H_{c2}(0)$ but also to find the precise position of the maximum of the Nernst signal, i.e., determine the ghost critical field. We emphasize that these are not fits to asymptotic expressions for the Nernst signal, which can lead to wrong conclusions about the ghost field since these maxima are typically not located in any asymptotic region of the phase diagram. Using our approach, we obtain the temperature dependence of the ghost field, which allows us to determine the scaling function in its dependence postulated in Ref. [15] and finally resolve this long-standing problem. We also illustrate why fitting the maxima extracted directly from experimental data cannot answer that question.

II. THE ISSUE OF THE GHOST FIELD TEMPERATURE DEPENDENCE

The analysis of the experimental data obtained from the HTS compound $\text{Pr}_{2-x}\text{Ce}_x\text{CuO}_4$ led the authors of Ref. [10] to the hypothesis that the temperature dependence of the “ghost critical field” is described by the expression

$$H_{\text{exp}}^*(T) = H_{c2}(0) \ln \frac{T}{T_{c0}}. \quad (1)$$

The prefactor in front of the logarithm with $H_{c2}(0)$ was determined by the observation that $H_{c2}(0)$ is the only empirical parameter that characterizes the strength of superconductivity. The authors stated that “the characteristic field scale encoded in superconducting fluctuations above T_c ” is equal to the field needed to kill superconductivity at $T = 0$ K, and we share this motivation. The argument justifying the logarithmic dependence of H^* on temperature was based on the statement that the maximum of the Nernst signal should correspond to the field where the magnetic length of a fluctuation Cooper pair L_H becomes equal to its “size.” We agree with the latter: in terms of the qualitative picture of superconducting fluctuations, one can see how, moving along the $H_{c2}(T)$ line, the Ginzburg-Landau long-wavelength scenario gradually transforms into the precursor of an Abrikosov vortex lattice: a set of clusters of rotating fluctuation Cooper pairs (FCPs) in magnetic field, which are relatively small (of size $\sim \xi_{\text{BCS}}$) [13,16]. Yet in order to practically apply this correct ideological idea, the authors of Refs. [8–11,17] extrapolated the Ginzburg-Landau (GL) expression for the FCP coherence length $\xi_{\text{FCP}}(T) = \xi_{\text{GL}}(T) \sim \xi_{\text{BCS}}/\sqrt{\ln \frac{T}{T_{c0}}}$, obtained with the assumption of closeness to the critical temperature [14], to the region of high temperatures, $T \gg T_{c0}$. Indeed, this procedure leads to Eq. (1).

However, at this point we need to stress that there is no theoretical justification for such an extrapolation procedure. Moreover, it leads to the obviously incorrect conclusion that at high temperatures, the size of FCPs becomes much less than ξ_{BCS} . The correlation length $\xi_{\text{FCP}}(T)$, identified with the fluctuation Cooper pair size, should be determined either from the pole of the two-particle Green’s function, or, equivalently, from the pole of the fluctuation propagator [14]. For arbitrary

temperatures and magnetic fields in an impure superconductor, the general form of the latter is

$$L_n^{(R)-1}(-i\omega, q_z^2) = -\rho_e \left[\ln \frac{T}{T_{c0}} + \psi \left(\frac{1}{2} + \frac{-i\omega + \Omega_H(n + \frac{1}{2}) + Dq_z^2}{4\pi T} \right) - \psi \left(\frac{1}{2} \right) \right]. \quad (2)$$

Close to the critical temperature, where $\ln \frac{T}{T_{c0}} \approx \frac{T-T_{c0}}{T_{c0}} = \epsilon \ll 1$, and in zero magnetic field, it takes the standard form of the diffusive mode, after expansion of the ψ function:

$$L(0, q^2) = -\frac{1}{\rho_e} \left(\epsilon + \frac{\pi D q^2}{8T} \right)^{-1}. \quad (3)$$

Analyzing the pole of this expression, $L^{-1}(0, q_0^2) = 0$, one indeed obtains $\xi_{\text{FCP}}(T \rightarrow T_{c0}) \sim q_0^{-1} \sim \xi_{\text{GL}}(\epsilon) \sim \xi_{\text{BCS}}/\sqrt{\epsilon}$. Yet far from the critical temperature, with the assumption that $\ln \frac{T}{T_{c0}} \gg 1$, the ψ function in Eq. (3) with a large argument should be replaced by its asymptotic logarithmic expression, and one obtains

$$L(0, q^2) = -\frac{1}{\rho_e} \ln^{-1} \left(\frac{Dq^2}{4\pi T_{c0}} \right). \quad (4)$$

The pole of this expression is given by $q_0^{-1} \sim \sqrt{\frac{4\pi T_{c0}}{D}}$, resulting in $\xi_{\text{FCP}}(T \gg T_{c0}) \sim q_0^{-1} \sim \xi_{\text{BCS}}$. Hence, the qualitative argumentation justifying Eq. (1) is unfounded.

In Ref. [15] the authors looked for an analytical expression for the ghost field by proposing a scaling argument based on the general expression for the fluctuation-induced Nernst signal (see Refs. [2,13,18]), valid over a wide range of temperatures and magnetic fields. It was noticed that the magnetic field, H , occurs only in combination with the temperature as H/T in this expression, while T also appears as parameter $\ln(T/T_{c0})$. This observation allowed them to obtain the following expression for the ghost field, which is very different from Eq. (1):

$$H_{\text{KV}}^*(T) = H_{c2}(0) \left(\frac{T}{T_{c0}} \right) \varphi \left(\ln \frac{T}{T_{c0}} \right), \quad (5)$$

where $\varphi(x)$ is some smooth function which satisfies the condition $\varphi(0) = 0$. It is easy to see that Eq. (5) coincides with Eq. (1) only in the very particular case of $\varphi(x) = x \exp(-x)$.

TABLE I. Asymptotic expressions (obtained in Ref. [2]) for fluctuation corrections to the Nernst signal in different domains of the phase diagram (see Fig. 3). Here $\mathfrak{N}_0 \equiv \frac{\pi \hbar}{k_B R_{\square}}$, $\tilde{h} = \frac{h - h_{c2}(t)}{h_{c2}(t)} \ll 1$, and $h_{c2}(0) = \frac{H_{c2}(0)}{H_{c2}(0)} = \frac{\pi^2}{8\gamma_E} = 0.69$ (see text).

Domain	t and h range	Description	$\pi \mathfrak{N}^{(1)}/\mathfrak{N}_0$
I	$h = 0, \epsilon \ll 1$	zero field, near T_{c0}	$\frac{2eH\xi_{\text{GL}}^2(T)}{3c} = \frac{h}{3c}$
II	$\epsilon \ll h \ll 1$	near T_{c0} , above the mirror reflected H_{c2} line	$1 - (\ln 2)/2$
III	$h - H_{c2}(t) \ll 1, \epsilon \ll 1$	near the H_{c2} line	$\frac{1}{\epsilon + h}$
IV	$t \ll \tilde{h}$	region of quantum fluctuations	$-\frac{2\gamma_E}{9} \frac{t}{h}$
V	$t^2/\ln(1/t) \ll \tilde{h} \ll t \ll 1$	quantum to classical	$\ln \frac{t}{\tilde{h}}$
VI	$\tilde{h} \ll t^2/\ln(1/t) \ll 1$	classical, near H_{c2} ($t \ll 1$)	$\frac{8\gamma_E^2}{3} \frac{t^2}{h(t)}$
VII	$t^2/\ln(1/t) \lesssim \tilde{h}(t) \ll 1$	classical, intermediate fields	$\frac{1}{\tilde{h}(t)} \left[1 + \frac{2H_{c2}(t)}{\pi^2 t} \frac{\psi''(\frac{1}{2} + \frac{2H_{c2}(t)}{\pi^2 t})}{\psi'(\frac{1}{2} + \frac{2H_{c2}(t)}{\pi^2 t})} \right]$
VIII	$\ln t \gtrsim 1, h \ll t$	high temperatures	$\frac{2}{3\pi^2} \frac{h}{t \ln t}$
IX	$h \gg \max\{1, t\}$	high magnetic fields	$\frac{\pi^2}{48} \frac{t}{h \ln h}$

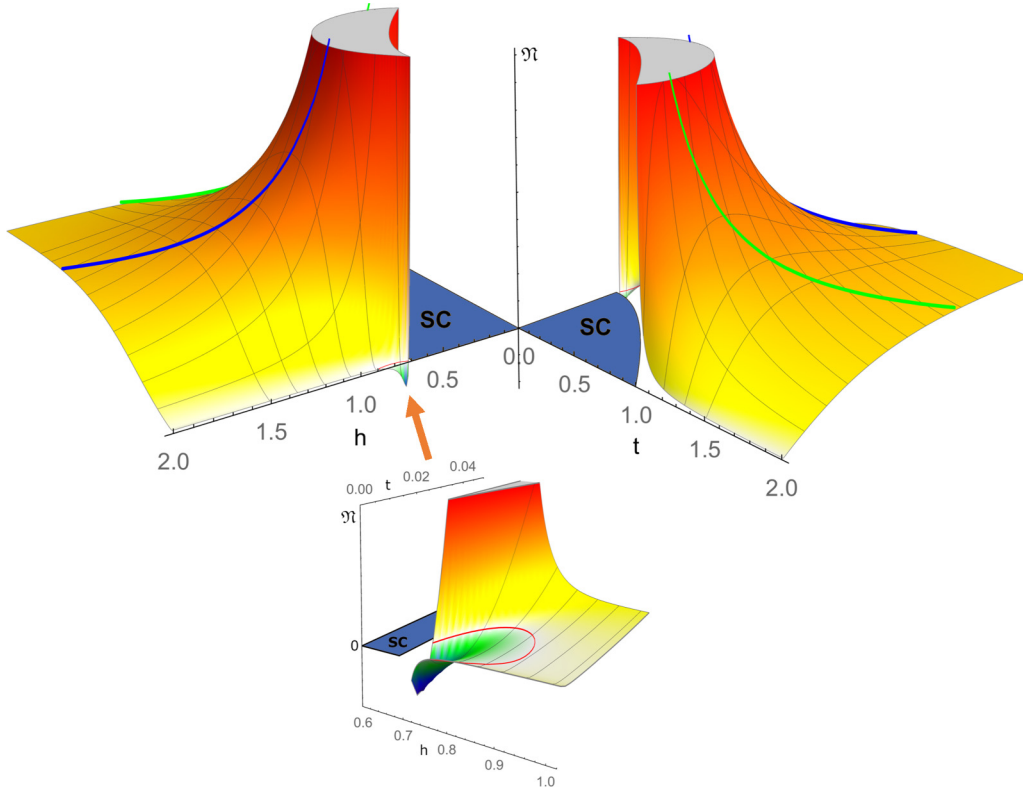


FIG. 1. The magnetic field and temperature dependence of the fluctuation part of the Nernst coefficient. Top left: A view of the $t = 0$ plane with the ghost temperature line in blue indicating the maximum of the Nernst coefficient for constant h . Top right: A view of the $h = 0$ plane with the ghost field line in green, indicating the maximum of the Nernst signal for constant fields. Bottom: Zoom of the quantum fluctuations (QF) region at $t = 0$ close to $h = h_{c2}$. The red line indicates the contour, where the Nernst signal is zero. In a very small area of the QF region, the Nernst coefficient becomes negative for $t \lesssim 0.02$ and $\tilde{h} \lesssim 0.15$ (see text).

Due to the extremely cumbersome nature of the general expression for the fluctuation-induced Nernst signal, none of the authors of Refs. [2,3,15] succeeded in obtaining an analytical expression for the temperature dependence of the ghost field valid far from the critical temperature. Yet simple equating of the asymptotic expressions valid at low fields and high temperatures, $\ln t \gtrsim 1$, $h \ll 1$ (see Table I, domain VIII),

$$\mathfrak{N}^{(fl)}(T, H) \sim \left(\frac{\xi_{\text{BCS}}^2}{L_{H_{c2}}^2} \right) \left(\frac{H}{H_{c2}(0)} \right) \left(\frac{T_{c0}}{T} \right) \ln^{-1} \frac{T}{T_{c0}} \quad (6)$$

(here $L_{H_{c2}}^2 = \frac{c}{2eH_{c2}(0)} \sim \xi_{\text{BCS}}^2$), and that valid for high fields, $h \gg \max\{1, t\}$ (see Table I, domain IX),

$$\mathfrak{N}^{(fl)}(T, H) \sim \left(\frac{L_{H_{c2}}^2}{\xi_{\text{BCS}}^2} \right) \left(\frac{T}{T_{c0}} \right) \left(\frac{H_{c2}(0)}{H} \right) \ln^{-1} \frac{H}{H_{c2}(0)}, \quad (7)$$

leads to the conclusion that at sufficiently high temperatures ($T \gtrsim T_{c0}$) the ghost critical field should grow as a function of

temperature almost linearly (with logarithmic accuracy):

$$H^*(T) \sim H_{c2}(0) \left(\frac{T}{T_{c0}} \right). \quad (8)$$

In Ref. [13], a general computational approach to the description of fluctuation phenomena in superconductors valid in the whole phase diagram, *numerical fluctuoscropy*, was presented. In the following we will apply this method for the determination of the true temperature dependence of the ghost field in the Nernst signal and its comparison with experimental data.

III. CONSISTENT DERIVATION OF THE GHOST FIELD

A. Theoretical foundation: Fluctuation-induced Nernst signal

The general expression for the fluctuation contribution to the Nernst signal of two-dimensional superconductors, valid beyond the line $H_{c2}(t)$, can be presented in a form suitable for the numerical analysis as [2,13,18]

$$\begin{aligned} \mathfrak{N}^{(fl)} = & \frac{\mathfrak{N}_0}{8\pi} \sum_{m=0}^{M_t} (m+1) \sum_{k=-\infty}^{\infty} \left\{ \left(\frac{\eta(2m+3)+|k|}{\mathcal{E}_m} + \frac{\eta(2m+1)+|k|}{\mathcal{E}_{m+1}} \right) (\mathcal{E}'_m - \mathcal{E}'_{m+1}) + 2\eta[\eta(2m+1)+|k|] \frac{\mathcal{E}''_m}{\mathcal{E}_m} + 2\eta[\eta(2m+3)+|k|] \frac{\mathcal{E}''_{m+1}}{\mathcal{E}_{m+1}} \right\} \\ & + 4\pi^2 \sum_{m=0}^{M_t} (m+1) \int_{-\infty}^{\infty} \frac{dx}{\sinh^2 \pi x} \left\{ \frac{\eta \text{Im} \mathcal{E}_m \text{Im} (\mathcal{E}_m + \mathcal{E}_{m+1}) + [\eta(m+1/2) \text{Im} \mathcal{E}_m + \frac{x}{2} \text{Re} \mathcal{E}_m] \text{Im} (\mathcal{E}_{m+1} + 2\eta \mathcal{E}'_m - \mathcal{E}_m)}{|\mathcal{E}_m|^2} \right\} \end{aligned}$$

$$\begin{aligned}
& + \frac{\eta \operatorname{Im} \mathcal{E}_{m+1} \operatorname{Im} (\mathcal{E}_m + \mathcal{E}_{m+1}) + [\eta(m+3/2) \operatorname{Im} \mathcal{E}_{m+1} + \frac{x}{2} \operatorname{Re} \mathcal{E}_{m+1}] \operatorname{Im} (\mathcal{E}_{m+1} + 2\eta \mathcal{E}'_{m+1} - \mathcal{E}_m)}{|\mathcal{E}_{m+1}|^2} + 2x \operatorname{Im} \ln \frac{\mathcal{E}_m}{\mathcal{E}_{m+1}} \\
& - 2 \frac{\operatorname{Im} (\mathcal{E}_m + \mathcal{E}_{m+1}) (\operatorname{Im} \mathcal{E}_m \operatorname{Im} \mathcal{E}_{m+1} + \operatorname{Re} \mathcal{E}_m \operatorname{Re} \mathcal{E}_{m+1})}{|\mathcal{E}_{m+1}|^2 |\mathcal{E}_m|^2} \left[\eta \left(m + \frac{3}{2} \right) \operatorname{Im} \mathcal{E}_{m+1} - \eta \left(m + \frac{1}{2} \right) \operatorname{Im} \mathcal{E}_m + \frac{x}{2} \operatorname{Re} (\mathcal{E}_{m+1} - \mathcal{E}_m) \right] \Bigg], \quad (9)
\end{aligned}$$

with $\mathfrak{N}_0 = \frac{ek_B R \square}{\hbar}$. Here the function

$$\mathcal{E}_m \equiv \mathcal{E}_m(t, h, |k|) = \ln t + \psi \left[\frac{|k| + 1}{2} + \eta \left(m + \frac{1}{2} \right) \right] - \psi \left(\frac{1}{2} \right) \quad (10)$$

is the denominator of the above-mentioned fluctuation propagator. Its derivatives with respect to the argument x are related to polygamma functions:

$$\begin{aligned}
\mathcal{E}_m^{(n)}(t, h, x) & \equiv \frac{\partial^n}{\partial x^n} \mathcal{E}_m(t, h, x) \\
& = 2^{-n} \psi^{(n)} \left[\frac{1+x}{2} + \eta \left(m + \frac{1}{2} \right) \right]. \quad (11)
\end{aligned}$$

We use here the convenient combination $\eta = \frac{4h}{\pi^2 t}$ of the dimensionless temperature $t = \frac{T}{T_{c0}}$ and magnetic field $h = \frac{H}{H_{c2}(0)}$. The latter is normalized by the value of the second critical field obtained by linear extrapolation of its temperature dependence near T_{c0} : $\tilde{H}_{c2}(0) = \Phi_0 / (2\pi \xi^2)$, where $\Phi_0 = \pi c / e$ is the magnetic flux quantum. The value of the magnetic field $\tilde{H}_{c2}(0)$ is $8\gamma_E / \pi^2$ times larger than Abrikosov's value for the second critical field $H_{c2}(0)$:

$$h = \frac{H}{\tilde{H}_{c2}(0)} = \frac{\pi^2}{8\gamma_E} \frac{H}{H_{c2}(0)} = 0.69 \frac{H}{H_{c2}(0)}. \quad (12)$$

In analogy to ϵ , which measures the closeness to T_{c0} in zero field, we introduce $\tilde{h}(t) = \frac{h - h_{c2}(t)}{h_{c2}(t)}$, where $\tilde{h}(0)$ measures the closeness to the true critical field at zero temperature. Despite the apparent divergence of Eq. (9) [we introduced the natural upper limit of the summation over Landau levels $M_t \sim (T_{c0}\tau)^{-1}$, with τ being the electron elastic scattering time], it, in fact, converges due to intricate cancellations in two divergent orders of the transport (Kubo) and magnetization current fluctuation contributions (see Refs. [2,15,19]). This can be verified by expanding all functions $\mathcal{E}_m^{(n)}(t, h, x)$ and their derivatives in Eq. (10) over Landau level differences in the limit of large numbers. Hence, the result of the summations does not depend on the cutoff parameter. This fact is also confirmed by the direct numerical evaluation.

B. Numerical analysis of the fluctuation-induced Nernst signal

The fluctuation contribution to the Nernst signal in the whole phase diagram beyond the $H_{c2}(t)$ line is presented in Fig. 1 as a surface plot in accordance to Eq. (9). Figure 2 shows selected isomagnetic and isothermal cuts of this surface plot. The asymptotic expressions for the Nernst signal in different domains of the phase diagram are summarized in Table I, and the corresponding domains are indicated in Fig. 3.

Close to the critical temperature T_{c0} (domains I–III), where fluctuations have Ginzburg-Landau thermal character, the Nernst signal is positive and grows in magnitude approaching the transition line [$h - H_{c2}(t) \ll 1$]. The “mirror field,” $h^{(m)}(t) = t - 1$, separates the linear and nonlinear regimes in the magnetic field dependence of the Nernst signal [20].

The isothermal Nernst signal graphs in Fig. 2(a) show the well-known nonmonotonous behavior of the Nernst signal for temperatures above T_{c0} . The dashed line connects the maxima for various fixed values of temperature, indicating the “ghost field temperature dependence,” which at sufficiently high tem-

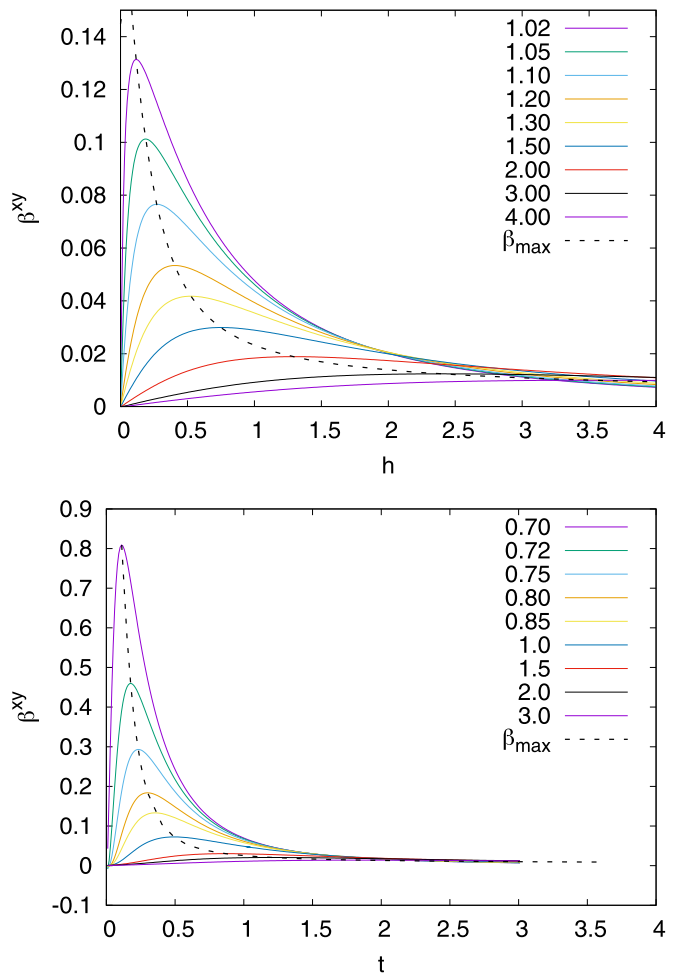


FIG. 2. Fluctuation-induced Nernst signal (a) as a function of magnetic field at constant temperatures (above T_{c0} , i.e., $t > 1$), where the reduced temperatures are indicated in the legend and the curve of maxima (dashed) is a function of temperature, and (b) as function of temperature at constant fields [above $h_{c2}(0)$], indicated in the legend, with the dashed maxima curve shown as a function of field.

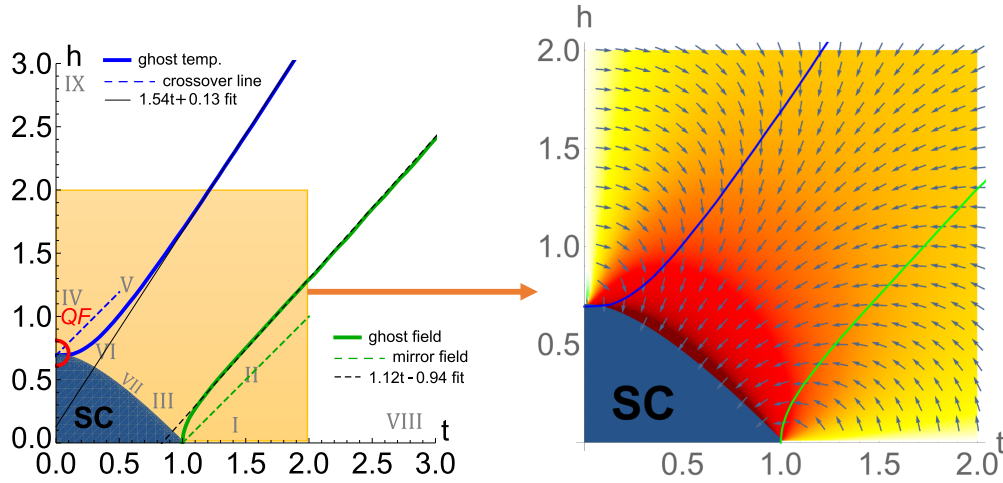


FIG. 3. Phase diagram (left panel) with the lines of the BCS second critical field $h_{c2}(t)$, the ghost field $h^*(t)$, the ghost temperature $t^*(h)$, the mirror field $h^{(m)}(t)$, and the crossover line from quantum to thermal fluctuations $t^{(qt)}(h)$. The regions of qualitatively different asymptotic behavior are indicated by roman numerals, which are explained in Table I. The region of quantum fluctuations is marked by “QF”; in this region the Nernst coefficient becomes negative. The shaded region is enlarged in the right panel, which shows both ghost lines with a density plot of the Nernst signal. In addition the (t, h) gradient of $\mathcal{N}^{(fl)}$ is indicated by a vector field. The ghost lines follow the vertical and horizontal gradients.

peratures is well described by the expression

$$h^*(t) \approx 1.12(t - 0.84), \quad (13)$$

as shown in Fig. 3. One can see that its linear dependence on temperature corresponds to our qualitative picture above and is quite different from the logarithmic law used in Refs. [10,11].

Of special interest is the study of the low-temperature regime of fluctuations, close to the upper critical field $H_{c2}(0)$ (domains IV–VI). Here a crossover line, $t^{(qt)}(h) = \tilde{h}$, exists, which separates the purely quantum regime at vanishing temperatures (domain IV) and the region of low temperatures, but where fluctuations already acquire thermal character (domain VI). It is interesting that in the quantum regime the fluctuation contribution to the Nernst signal is negative in a very small t - h area, where it depends linearly on temperature and diverges as \tilde{h}^{-1} when approaching the transition point (see the inset in Fig. 1). This change in the sign in the fluctuation thermoelectric response is similar to the negative fluctuation conductivity close to the quantum phase transition in the vicinity of $H_{c2}(0)$, found in Ref. [21]. These negative values comes from the diffusion coefficient renormalization contribution, which exceeds the positive, but fading away, Aslamasov-Larkin (AL) term in this region. In the quantum-to-classical crossover region (domain V), the Nernst signal becomes positive and less singular ($\sim \ln \frac{t}{\tilde{h}}$). Increasing the temperature, one goes over into the region of thermal fluctuations (domain VI) and sees that the Nernst signal continues to grow as $\sim t^2/\tilde{h}$.

In the isomagnetic Nernst signal plots above the second critical field, shown in Fig. 2(b), one sees, like in the situation above T_{c0} , that the Nernst signal temperature dependence at a fixed field is nonmonotonous and has a maximum. The line connecting these maxima can be called the “ghost temperature

line,” and it is well described by the linear dependence

$$t^*(h) \approx 0.65(h - 0.13) \quad (14)$$

for $h > 1$ (see Fig. 3, the $1.54t + 0.13$ fit).

In the following we will use these insights and complete expression, Eq. (9), for the Nernst signal to fit experimental data, allowing us to perform a characterization of the superconducting material. In particular, we can extract the values of T_{c0} and $H_{c2}(0)$ without using any “artificial” convenience criteria (like the half width of the transition region, 90% of the resistance decay, the temperature where the derivative of the resistance is maximal or has an inflection point, etc.). In a “simplified” version one can just use the ghost field and ghost temperature lines [Eqs. (13) and (14)] for fitting instead of the nontrivial *fluctuoscropy*, the full fitting procedure of the Nernst signal.

IV. $\text{Nb}_x\text{Si}_{1-x}$ EXPERIMENTS

In order to verify our theoretical studies, measurements on two stoichiometrically identical samples of $\text{Nb}_x\text{Si}_{1-x}$ were performed, labeled samples 1 and 2 in the following. The Nb concentration x was fixed at $x = 0.15$. These amorphous film samples were prepared under ultrahigh vacuum by electron-beam coevaporation of Nb and Si with precise control over concentrations and deposited on sapphire substrates. Such films typically undergo a metal-insulator transition when x decreases.

The two samples have different thicknesses, which mostly controls their critical parameters since the nominal concentration is the same: Sample 1 (2) was 12.5 (35) nm thick, its experimental midpoint $T_{c0}^{(\text{exp})}$ was 0.165 (0.380) K (resistively measured in zero field), and its upper critical field $H_{c2}^{(\text{exp})}(0)$ was 0.36 (0.91) T. The zero-temperature coherence lengths for the samples are 19.7 and 13 nm, respectively.

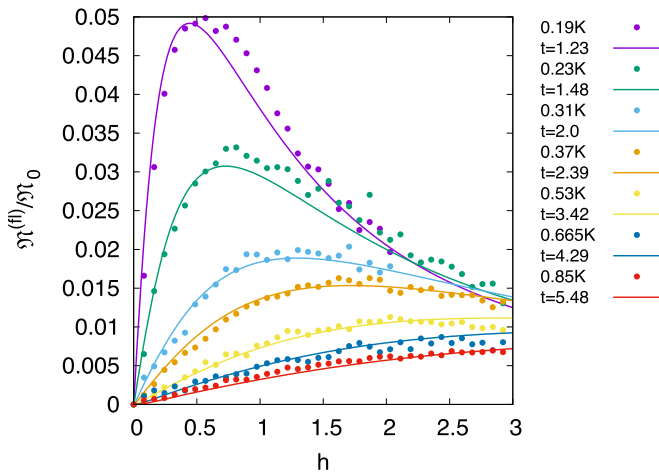


FIG. 4. Fit of the Nernst signal for Nb_{0.15}Si_{0.85} (sample 1) to Eq. (9). The found fitting parameters are $T_{c0} = 0.165$ K, $H_{c2}(0) = 0.36$ T.

The Nernst coefficient is obtained by measuring the thermoelectric and electric coefficients of both samples in a dilution fridge using a resistive heater, two RuO₂ thermometers, and two lateral contacts. Partial data were published in Refs. [8,9]. At $T \sim 0.19$ K, the dc voltage resolution for our setup was 1 nV, and temperature resolution was 0.1 mK. The results are discussed below.

V. NERNST SIGNAL FLUCTUOSCOPY OF Nb_{0.15}Si_{0.85} AND OTHER MATERIALS

As already noted, in previous studies the dependence of the fluctuation contribution to the Nernst signal on magnetic field and temperature above the critical one was fitted [12] by asymptotic expressions and interpolations between them [1–4] with limited accuracy, which also does not allow for a consistent extraction of the ghost lines. Here we use the general expression (9) for detailed numerical analysis and high-precision fitting of experimental data in the whole t - h plane without the interpolation procedure.

In Figs. 4 and 5 one can see how accurately Eq. (9) fits the experimental data of two Nb_{0.85}Si_{0.15} samples using only two fitting parameters: T_{c0} and $H_{c2}(0)$. The values of the fitting parameters for sample 1 are $T_{c0}^{(\text{theo})} = 0.165$ K and $H_{c2}^{(\text{theo})}(0) = 0.36$ T.

Similarly, the fits of the measurements obtained for sample 2 give values of the critical temperature and second critical field close to their experimentally estimated meanings: $T_{c0}^{(\text{theo})} = 0.36$ K and $H_{c2}^{(\text{theo})}(0) = 0.7$ T.

The observation that the theoretical value of the critical temperature is lower than the experimentally obtained value is in agreement with previous findings that T_{c0} is typically overestimated when using traditional empirical methods, which are (visually) convenient but only approximate (see Ref. [22] for a detailed comparison in the case of fluctuation conductivity measurements).

The dependence of the position of the maximum in the Nernst signal $\mathfrak{N}^{(fl)}(h)$ versus temperature for Nb_{0.85}Si_{0.15} is shown in Fig. 6, which demonstrates both the numerically obtained theoretical curve and the values extracted from the

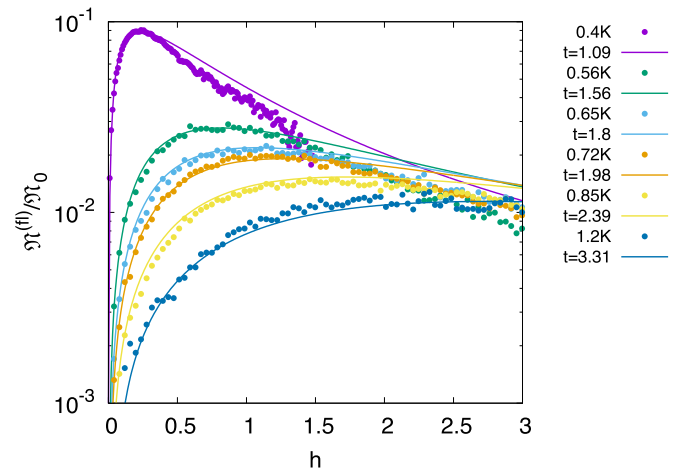


FIG. 5. Fit of the Nernst signal for Nb_{0.15}Si_{0.85} (sample 2) to Eq. (9), shown in half-logarithmic representation. The found fitting parameters are $T_{c0} = 0.36$ K, $H_{c2}(0) = 0.7$ T, which are close to the experimentally estimated values.

experimental data. One can see that the behavior of $h^*(t)$ obtained from the numerical study of the extremum of Eq. (9) is strongly nonlinear close to T_{c0} but becomes linear as function of temperature quickly and can be described by Eq. (13). However, we note that the error bars of the experimentally obtained ghost field become quite large due to the broadness of the maxima, such that the theoretical curve lies well within the error. Similar results are obtained for sample 2.

Besides the two Nb_xSi_{1-x} samples, we also analyzed several other available Nernst signal measurements using Nernst fluctuoscropy. In Fig. 7, the temperature dependence of the normalized ghost field [scaled by $H_{c2}(0)$] from two different experiments (squares and crosses) is compared to the numerically obtained ghost field line from Eq. (9) (solid green line) and to the empirical $\sim \ln(t)$ (thin or-

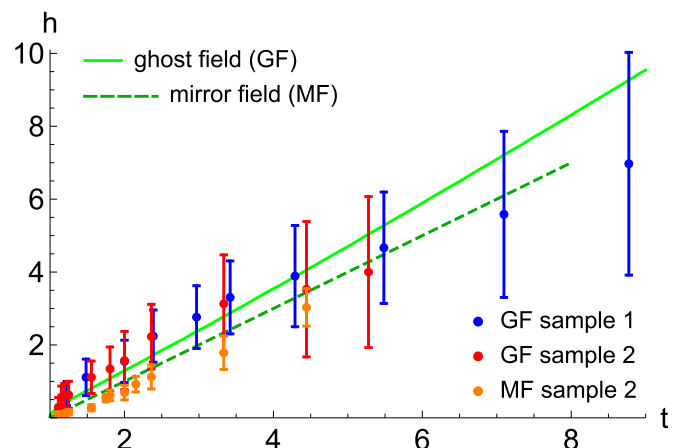


FIG. 6. Numerically evaluated ghost field curve $h^*(t)$ from Eq. (9) (solid green line) and the mirror field (dashed green line). Extracted ghost field from experimental data scaled by fitting parameters with error bars for both samples and the extracted mirror field for sample 2, when the Nernst coefficient starts to deviate from linear behavior. As one can see, the error bars for the ghost field become larger for larger temperatures since the maxima become very broad.

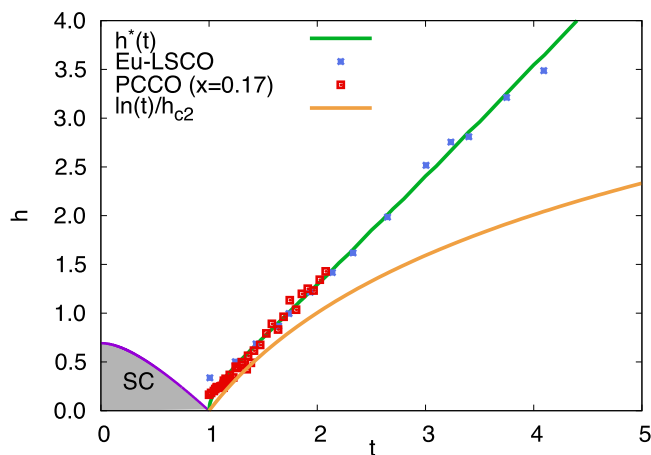


FIG. 7. Fit of the ghost field data for Eu-LSCO and PCCO to the numerically evaluated curve $h^*(t)$ from Eq. (9) and comparison to a logarithmic dependence.

ange line). The experimental data on Eu-doped LSCO, $\text{La}_{1.8-x}\text{Eu}_{0.2}\text{Sr}_x\text{CuO}_4$ (Eu-LSCO), (blue crosses) are taken from Ref. [17] [Fig. 3(b)], and the data on $\text{Pr}_{2-x}\text{Ce}_x\text{CuO}_4$ (PCCO) at doping level $x = 0.17$ (overdoped sample, red squares) are from Ref. [10] (their Fig. 10). One sees that the experimental findings fit the theoretical curve very well and, in particular, follow the linear behavior given by Eq. (13).

Finally, we also applied the numerical Nernst fitting procedure to the heavy-fermion superconductor URu_2Si_2 [11], where we used the measured Nernst signal data at different temperatures (Fig. 4 in Ref. [11]) and fitted $\mathfrak{N}^{(fl)}(h)$ with fitting parameters $T_{c0} = 1.14$ K, which is slightly lower than the empirically determined value of 1.45 K, and $H_{c2}(0) = 1.11$ T, which is close to the values found in previous experimental works [23–25]. The result is shown in Fig. 8 [26]. Based on these Nernst signal fittings, we extracted the positions of maxima (the values of ghost fields) and compare them to the experimentally extracted values in the inset of Fig. 8 [27].

VI. DISCUSSION

We presented a complete analysis of the magnetic field and temperature dependence of the fluctuation-induced Nernst signal in a large variety of superconductors ranging from conventional to unconventional ones as long as they are described by the BCS model. That also includes overdoped cuprate superconductors, whose properties can be mostly described by the Gaussian approximation in the fluctuation region.

We developed a numerical fluctuation spectroscopy approach based on the complete expression of the fluctuation contribution to the Nernst signal in the whole range of temperatures and magnetic fields and applied it to experi-

mental Nernst signal measurements. Both magnetic field and temperature dependence of the Nernst signal data are fitted

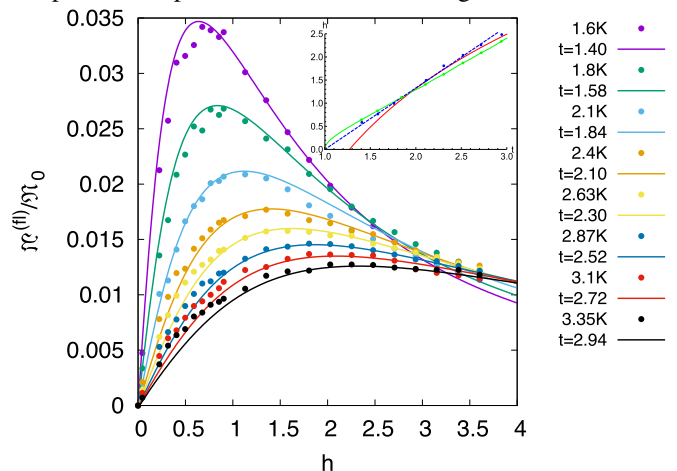


FIG. 8. Fit of the normalized Nernst signal vs magnetic field measurements on the heavy-fermion superconductor URu_2Si_2 [11] to Eq. (9) for different temperatures. The fitting parameters are $T_{c0} = 1.14$ K and $H_{c2}(0) = 1.11$ T. Inset: the ghost field measurements (blue circles) compared to the universal curve following Eq. (9) (green) and the logarithmic [Eq. (1)] fitting (red). In addition we added a linear fit to the experimental data (dashed blue line).

with very good accuracy using only two fitting parameters: the superconducting temperature T_{c0} and the upper critical field $H_{c2}(0)$.

Our approach predicts a linear temperature dependence for the ghost critical field well above T_{c0} , contrary to previous heuristic arguments resulting in a logarithmic dependence on temperature [10]. Within the errors of the experimental data, this linearity is, indeed, observed in many superconductors far from T_{c0} . From a technical point of view we note that the maxima of the Nernst signal become very shallow at large temperatures, which makes their extraction from experimental data very difficult. Therefore, the seemingly simple approach to the determination of the critical temperature T_{c0} and critical field $H_{c2}(0)$ from the fitting of the ghost field should be done with care, giving high-temperature points lower weight.

ACKNOWLEDGMENTS

We thank K. Behnia and M. Serbyn for valuable discussions. This work was supported by the U.S. Department of Energy, Office of Science, Basic Energy Sciences, Materials Sciences and Engineering Division. A.A.V. acknowledges the hospitality of Argonne National Laboratory, Northern Illinois University, and support from the European Union's Horizon 2020 research and innovation program under the Grant Agreement No. 731976 (MAGENTA).

[1] I. Ussishkin, S. L. Sondhi, and D. A. Huse, *Phys. Rev. Lett.* **89**, 287001 (2002).

[2] M. N. Serbyn, M. A. Skvortsov, A. A. Varlamov, and V. Galitski, *Phys. Rev. Lett.* **102**, 067001 (2009).

[3] K. Michaeli and A. M. Finkelstein, *Europhys. Lett.* **86**, 27007 (2009).

[4] A. Levchenko, M. R. Norman, and A. A. Varlamov, *Phys. Rev. B* **83**, 020506(R) (2011).

- [5] A. Sergeev, M. Reizer, and V. Mitin, *Phys. Rev. Lett.* **106**, 139701 (2011).
- [6] M. N. Serbyn, M. A. Skvortsov, A. A. Varlamov, and V. Galitski, *Phys. Rev. Lett.* **106**, 139702 (2011).
- [7] Z. A. Xu, N. P. Ong, Y. Wang, T. Kakeshita, and S. Uchida, *Nature (London)* **406**, 486 (2000).
- [8] A. Pourret, H. Aubin, J. Lesueur, C. Marrache-Kikuchi, L. Berge, L. Dumoulin, and K. Behnia, *Nat. Phys.* **2**, 683 (2006).
- [9] A. Pourret, H. Aubin, J. Lesueur, C. A. Marrache-Kikuchi, L. Bergé, L. Dumoulin, and K. Behnia, *Phys. Rev. B* **76**, 214504 (2007).
- [10] F. F. Tafti, F. Laliberté, M. Dion, J. Gaudet, P. Fournier, and L. Taillefer, *Phys. Rev. B* **90**, 024519 (2014).
- [11] T. Yamashita, Y. Shimoyama, Y. Haga, T. Matsuda, E. Yamamoto, Y. Onuki, H. Sumiyoshi, S. Fujimoto, A. Levchenko, T. Shibauchi, and Y. Matsuda, *Nat. Phys.* **11**, 17 (2015).
- [12] K. Behnia and H. Aubin, *Rep. Prog. Phys.* **79**, 046502 (2016).
- [13] A. A. Varlamov, A. Galda, and A. Glatz, *Rev. Mod. Phys.* **90**, 015009 (2018).
- [14] A. Larkin and A. Varlamov, *Theory of Fluctuations in Superconductors*, International Series of Monographs on Physics (Oxford University Press, Oxford, 2009).
- [15] A. V. Kavokin and A. A. Varlamov, *Phys. Rev. B* **92**, 020514(R) (2015).
- [16] A. Glatz, A. A. Varlamov, and V. M. Vinokur, *Europhys. Lett.* **94**, 47005 (2011).
- [17] J. Chang, N. Doiron-Leyraud, O. Cyr-Choiniere, G. Grissonnanche, F. Laliberte, E. Hassinger, J.-P. Reid, R. Daou, S. Pyon, T. Takayama, H. Takagi, and L. Taillefer, *Nat. Phys.* **8**, 751 (2012).
- [18] M. Serbyn, M.S. thesis [in Russian], Moscow Institute of Physics and Technology, 2009.
- [19] Y. N. Obraztsov, *Fiz. Tverd. Tela* **6**, 414 (1964) [*Sov. Phys. Solid State* **6**, 331 (1964)].
- [20] The notion of “mirror-symmetric field” was introduced by Buzdin and Dorin [28] in the study of the nonlinear fluctuation magnetization close to the critical temperature and arbitrary magnetic fields. It has the meaning of a crossover line, which separates linear and nonlinear regimes of the fluctuation magnetization, conductivity, and other characteristics [14] in the phase diagram. Well before, the exact same meaning of the crossover line between linear and nonlinear regimes in fluctuation conductivity was investigated by Kapitulnik *et al.* [29], who called it the “ghost field.” In the 2000s, after the discovery of the non-monotonous behavior of the fluctuation-induced Nernst signal as a function of magnetic field [8,9], the name “ghost field” was attributed to the value of magnetic field corresponding to its maximum. Following these works and others [10] the term “ghost field” was henceforth used in the latter sense. It is clear that the “mirror field” is always smaller the “ghost field” $h^*(t)$, as demonstrated in Fig. 6.
- [21] V. M. Galitski and A. I. Larkin, *Phys. Rev. Lett.* **87**, 087001 (2001).
- [22] T. I. Baturina, S. V. Postolova, A. Y. Mironov, A. Glatz, M. R. Baklanov, and V. M. Vinokur, *Europhys. Lett.* **97**, 17012 (2012).
- [23] W. K. Kwok, L. E. DeLong, G. W. Crabtree, D. G. Hinks, and R. Joynt, *Phys. Rev. B* **41**, 11649 (1990).
- [24] V. V. Moshchalkov, F. Aliev, V. Kovachik, M. Zalyaljutdinov, T. T. M. Palstra, A. A. Menovsky, and J. A. Mydosh, *J. Appl. Phys.* **63**, 3414 (1988).
- [25] E. A. Knetsch, J. J. Petersen, A. A. Menovsky, M. W. Meisel, G. J. Nieuwenhuys, and J. A. Mydosh, *Europhys. Lett.* **19**, 637 (1992).
- [26] Note that the Nernst signal curve measured at 2.1 K is labeled by 2.0 K in Fig. 4 of Ref. [11].
- [27] Our fitting procedure revealed a discrepancy in the temperature values given in Fig. 4 of Ref. [11]. We contacted one of the authors, who confirmed that $T = 2.00$ K should be, in fact, $T = 2.10$ K.
- [28] A. Buzdin and V. Dorin, in *Fluctuation Phenomena in High Temperature Superconductors*, edited by M. Ausloos and A. A. Varlamov, NATO ASI Series (3. High Technology), Vol. 32 (Springer, Dordrecht, 1997).
- [29] A. Kapitulnik, A. Palevski, and G. Deutscher, *J. Phys. C* **18**, 1305 (1985).